Acta Crystallographica Section D
Biological Crystallography
ISSN 0907-4449

Purification, crystallization and preliminary X-ray crystallographic analysis of ATP-phosphoribosyltransferase from *Escherichia coli*

Bernhard Lohkamp,[a] John R. Coggins[a] and Adrian J. Lapthorn[b]*

[a]Division of Biochemistry and Molecular Biology, Institute of Biomedical and Life Sciences, University of Glasgow, Glasgow G12 8QQ, Scotland, and [b]Department of Chemistry, University of Glasgow, Glasgow G12 8QQ, Scotland

Correspondence e-mail: adrian@chem.gla.ac.uk

Received 5 May 2000
Accepted 11 August 2000

ATP-phosphoribosyltransferase (ATP-PRT) from *Escherichia coli* has been purified and crystals were obtained by the vapour-diffusion method using sodium tartrate as a precipitant. Dynamic light scattering was used to assess conditions for the monodispersity of the enzyme. The crystals are trigonal, space group *R*32, with unit-cell parameters $a = b = 133.6$, $c = 114.1$ Å (at 100 K), and diffract to 2.7 Å on a synchrotron X-ray source. The asymmetric unit is likely to contain one molecule, corresponding to a packing density of 2.9 $Å^3\ Da^{-1}$. A model for the quaternary structure is proposed based on the crystallographic symmetry.

1. Introduction

In microorganisms and plants, histidine is synthesized in ten steps by the enzymes of the histidine pathway. Eight enzymes are encoded on eight genes (*hisG{IE}AHFBCD*) often arranged as one operon (*his* operon). Three of the enzymes are bifunctional (*hisIE*, *hisD*, *hisB*) and two form a multienzyme complex catalysing one reaction (*hisH*, *hisF*) (see, for example, Alifano *et al.*, 1996). The pathway leads from 5-phosphoribosyl 1-pyrophosphate (PRPP) and ATP to histidine.

The initial substrates of the histidine pathway, PRPP and ATP, play a key role in intermediary and energy metabolism. Furthermore, they link the histidine pathway to the biosynthesis of folates, purines, pyrimidines, pyridine nucleotides and tryptophan.

The first enzyme of the pathway, ATP-phosphoribosyltransferase (ATP-PRT; E.C. 2.4.2.17) encoded by the *hisG* gene, catalyses the condensation of ATP and PRPP to form *N*′-5′-phosphoribosyl-ATP (PRATP). In addition to its catalytic function, it has been shown to be involved in several aspects of the regulation of histidine biosynthesis (Ames *et al.*, 1961). ATP-PRT binds to the *his* operon and to histidyl-tRNA and is feedback inhibited by the end-product of the pathway, histidine (Voll *et al.*, 1967). Owing to these regulatory functions and the connection of the histidine pathway to other biosynthetic and metabolic pathways, ATP-PRT plays an important part in the regulation of growth.

From the primary structure of ATP-PRT, the molecular weight is deduced as 33 367 Da for the 299 amino acids. Experimentally determined molecular weights in the literature describe various oligomeric states of ATP-PRT. Ultracentrifugation and gel separation have shown that the enzyme is in equilibrium between its active dimeric form, inactive hexameric form and higher aggregates (Klungsøyr & Kryvi, 1971; Tebar *et al.*, 1973). The hexameric form is stabilized by histidine, AMP, PRATP, high concentrations of ATP and high enzyme concentration (Klungsøyr & Kryvi, 1971; Kryvi & Klungsøyr, 1971). The second substrate PRPP seems to dissociate higher aggregates, resulting in an increase in the concentration of dimers (Tebar *et al.*, 1973).

The secondary structure of ATP-PRT has been investigated using CD spectroscopy (Kryvi, 1973). At that time it was proposed to consist of about 33% α-helix and 20–30% β-sheet, with no change observed when the inhibitors AMP and/or histidine were bound. Furthermore, it was proposed that the first 120 residues of ATP-PRT contain a nucleotide-binding fold arranged in a $\beta\alpha\beta\alpha\beta\beta\alpha\beta\alpha\beta$ pattern (Argos *et al.*, 1983). To our knowledge, no comparison of ATP-PRT with other phosphoribosyltransferases (PRT) of which structures are now known has been made (see, for example, Focia *et al.*, 1998).

In common with a number of amino-acid biosynthetic pathways, the histidine pathway is present in bacteria, fungi and plants but absent in mammals. This makes it a good target for the development of antimicrobial and antifungal drugs as well as herbicides (Mousdale & Coggins, 1991). A variety of selective inhibitors for the histidine pathway are known and are used commercially as herbicides (Mori *et al.*, 1995). These herbicidal compounds all inhibit imidazoleglycerol-phosphate dehydratase, the product of the *hisB* gene. Knowledge of the structure of ATP-PRT will help with the understanding of its function and will provide a basis for the development of antimicrobial drugs and herbicides.

Table 1
Dynamic light-scattering measurements of *E. coli* ATP-PRT in the presence of different additives.

The hydrodynamic radius represents the median particle size present in the sample cell. The polydispersity value indicates the standard deviation of the spread of particle sizes about the reported average radius. A rise in polydispersity in relation to the average radius represents greater spread in the size distribution. The estimated M_w is calculated from the hydrodynamic radius (R_H) using an empirically derived relationship between the R_H and M_w values for a number of well characterized globular proteins in buffered solution. All experiments were conducted in 50 m*M* Tris–HCl buffer at pH 7.5 in the presence of 100 m*M* KCl unless otherwise stated. Samples containing PPRP and ATP were incubated at room temperature for 10 min to form PRATP.

Additives	Hydrodynamic radius (nm)	Polydispersity (nm)	Estimated M_w (kDa)	Conclusion
None (no KCl)	7.3	0.3	369	Polydisperse
None	6.9	1.0	321	Polydisperse
AMP (0.4 m*M*)	5.5	0.7	186	Polydisperse
Histidine (5 m*M*)	5.7	0.9	197	Polydisperse
Histidine (5 m*M*) + AMP (1 m*M*)	5.3	1.0	170	Polydisperse
PRPP (1 m*M*) + ATP (5 m*M*) + $MgCl_2$ (10 m*M*)	5.5	1.5	184	Polydisperse
PRPP (1 m*M*) + ATP (5 m*M*) + $MgCl_2$ (10 m*M*) + histidine (5 m*M*)	5.6	1.6	190	Polydisperse

2. Enzyme purification

ATP-PRPP from *E. coli* was overexpressed in *E. coli* B834(DE3)pLysS to 30–40% of the total cellular protein using a T7 RNA polymerase expression system (Studier & Moffatt, 1986). Cultures were grown in LB medium at 315 K to an optical density of 0.6 at 600 nm. Overexpression of protein was induced by addition of IPTG to a final concentration of 0.4 m*M*. Bacterial growth was continued for 4 h prior to harvesting the cells.

The cells (5.3 g wet weight) suspended in 20 ml of 50 m*M* Tris–HCl pH 7.5 containing 0.4 m*M* DTT and two protease inhibitor tablets (EDTA-free; Boehringer-Mannheim) per 100 ml (buffer *A*) were broken by two passes through a French pressure cell at 6.5 MPa. This material was then diluted with 40 ml buffer *A* and centrifuged at 18 000 rev min^{-1} for 1 h. ATP-PRT was purified from the resulting cell-free extract. All subsequent steps were performed at 277 K.

The supernatant was applied to a DEAE–Sephacel anion-exchange column (21 × 14 cm diameter, flow rate 60 ml h^{-1}) equilibrated in 50 m*M* Tris–HCl pH 7.5 containing 0.4 m*M* DTT and one protease inhibitor tablet per litre (buffer *B*). The column was then washed with the same buffer until the A_{280nm} of the eluate was less than 0.3. ATP-PRT was eluted with a linear gradient of 0–500 m*M* KCl in 700 ml buffer *B* (flow rate 30 ml h^{-1}) and 10 ml fractions collected and assayed as described in Martin *et al.* (1971). Fractions containing ATP-PRT activity were pooled and dialysed overnight against buffer *B*.

The protein was loaded on a dye column (Reactive Green 19, Sigma; 8.5 × 2.1 cm diameter, flow rate 40 ml h^{-1}) equilibrated in buffer *B*. The column was then washed with 50 ml buffer *B* and ATP-PRT was eluted with a linear gradient (250 ml) of 200–950 m*M* KCl in buffer *B*. The flow rate was 40 ml h^{-1} and 10 ml fractions were collected and assayed. Fractions containing ATP-PRT activity were pooled, dialysed overnight against buffer *B* and concentrated by ultrafiltration. At this stage, the enzyme precipitated at high concentrations, but no substantial amount of enzyme was lost owing to its irreversible precipitation.

The concentrated enzyme solution was applied to a Sephacryl S200 (superfine grade) column (170 × 1.5 cm diameter, flow rate 15 ml h^{-1}) that had been equilibrated with buffer *B* containing 500 m*M* KCl. The enzyme was eluted with buffer *B* containing 500 m*M* KCl (flow rate 10 ml h^{-1}, 10 ml fractions). Fractions containing ATP-PRT activity were dialysed against buffer *B* containing 50%(*v*/*v*) glycerol prior to long-term storage at 253 K.

3. Dynamic light scattering

Experiments were carried out using a DYNA-PRO 801 dynamic light-scattering/molecular-sizing instrument (Protein Solutions, Buckinghamshire, England). Protein solutions (1 mg ml^{-1}) were in 50 m*M* Tris–HCl pH 7.5, but several other buffers and pHs were also assessed. Dynamic light-scattering experiments were carried out to determine which combination of product and cofactor were appropriate to obtain a monodisperse enzyme solution. Monodispersity is not an infallible indicator that diffraction-quality crystals can be obtained from a protein; instead, it reflects the observation that monodisperse protein solutions have a much higher probability of producing crystals than those which are not (Ferré-D'Amaré & Burley, 1997). Dynamic light-scattering experiments on ATP-PRT were performed using several conditions and in the presence of different inhibitors (Table 1). It was shown that monodispersity could not be achieved in the presence of any of the probed additives. The lowest value for polydispersity was obtained using 0.4 m*M* AMP, with a resultant molecular weight estimated as 186 000 Da. This is about 10% lower than the M_w of six monomers, but consistent with the expected hexameric state of the enzyme. Other additives, such as histidine and PRATP, gave similar molecular weights and hydrodynamic radii but higher polydispersity. Furthermore, the solubility of the enzyme was found to be greatly increased in the presence of AMP (from about 5 mg ml^{-1} in buffer to at least 20 mg ml^{-1}). In the light of these results, crystallization trials were carried out in the presence and absence of AMP.

4. Crystallization

The enzyme was stored in 50%(*v*/*v*) glycerol, which was removed by exhaustive dialysis against 50 m*M* Tris–HCl pH 7.5 containing 0.4 m*M* DTT. The enzyme was concentrated to 11 mg ml^{-1} in 50 m*M* Tris–HCl pH 7.5, 0.4 m*M* DTT and 2 m*M* AMP using Centricon-10 centrifugal concentrators (Amicon, Stonehouse, Gloucestershire, England).

Crystallization experiments were performed at 293 K using the sitting-drop vapour-diffusion technique. An exhaustive

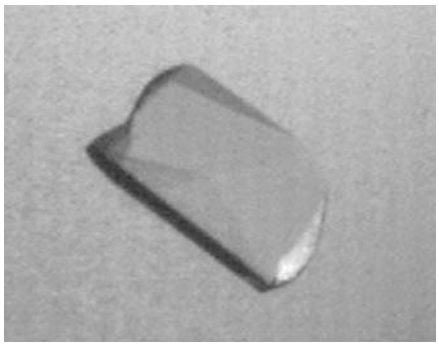

Figure 1
A crystal of ATP-PRT from *E. coli*. The crystal is approximately 0.3 × 0.2 × 0.2 mm in size (crystal form I).

Table 2
Statistics for the X-ray data processed in *R*32.

d_{min} (Å)	R_{sym} (I)	(I/σ)	No. of unique reflections	Completeness (%)	Multiplicity (%)
5.82	0.041	38.2	1099	95.6	6.3
4.62	0.061	39.1	1104	99.6	6.6
4.03	0.055	36.7	1098	99.9	6.7
3.66	0.050	32.2	1094	100.0	6.7
3.40	0.071	23.6	1079	100.0	6.7
3.20	0.120	14.5	1075	100.0	6.7
3.04	0.180	10.4	1092	100.0	6.7
2.91	0.293	6.4	1076	100.0	6.7
2.80	0.469	4.3	1077	100.0	6.7
2.70	0.668	3.1	1066	100.0	6.7
Total	0.049	18.0	10860	99.5	6.7

set of conditions, comprising commercially available and local sparse-matrix screens (Jancarik & Kim, 1991; Cudney *et al.*, 1994), were tried. Initial crystals were obtained from various conditions, mostly in the presence of AMP. Optimization of these crystallization conditions was most successful for a single condition which led to the final conditions of 1.3 *M* sodium tartrate, 50–200 m*M* $MgCl_2$, 100 m*M* citrate buffer pH 5.6 and protein in the presence of 2 m*M* AMP (crystal form I). Typically, 1–2 µl of protein (10 mg ml^{-1}) was mixed with an equal volume of the reservoir solution. Crystals appeared after 3–4 d and continued to grow as trigonal prisms to maximum dimensions of 0.3 × 0.2 × 0.2 mm (Fig. 1). A second crystal form was derived using 1.36–1.44 *M* ammonium sulfate, 0–0.3 *M* sodium chloride, 100 m*M* HEPES buffer pH 7.5 and protein in the presence of 2 m*M* AMP. Round-shaped crystals appeared after 4–5 d and grew to maximum dimensions of about 0.2 × 0.2 × 0.2 mm (crystal form II).

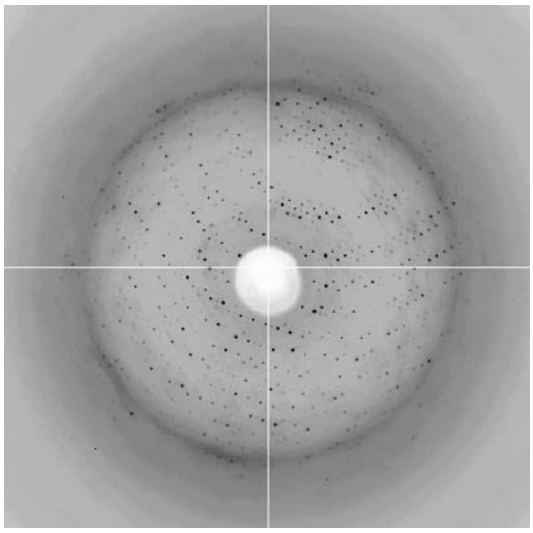

Figure 2
A typical diffraction pattern from ATP-PRT collected on beamline 9.6 at Daresbury synchrotron.

5. X-ray analysis

The X-ray diffraction data were collected on beamline 9.6 at the SRS, Daresbury Laboratory using a wavelength of 0.87 Å and a ADSC Quantum-4 CCD detector. The crystals were radiation sensitive and therefore cryocooling was essential. Crystals were loop-mounted in a cryoprotectant containing 15%(*v*/*v*) glycerol and cryocooled to 100 K using an Oxford Cryosystems Cryostream. A native data set to 2.7 Å resolution was collected using 1° oscillation frames from crystal form I (Fig. 2). Data were processed with *DENZO* and scaled with *SCALEPACK* (Otwinowski & Minor, 1997). From autoindexing in *DENZO*, the crystals were found to index in a primitive rhombohedral lattice corresponding to space group *R*3, with unit-cell parameters $a = b = 133.6$, $c = 114.1$ Å. Indexing with the higher symmetry space group *R*32 resulted in comparable merging *R*-factor statistics (Table 2). For *R*32, only one monomer per asymmetric unit leads to an acceptable packing density V_M of 2.95 Å^3 Da^{-1}, which corresponds to a solvent content of 58% (Matthews, 1968).

Crystal form II diffracted to only 3.7 Å; from a single frame, processing was performed as described above. The crystal symmetry was determined to be primitive rhombohedral, with unit-cell parameters $a = b = 132.6$, $c = 113.8$ Å. Because of the similar unit-cell parameters and the identical lattice, we presume that crystal form II also belongs to space group *R*32.

So far there are two different types of PRT structures known and another one predicted. Several reported structures, *e.g.* uracil PRT, show the type I fold of a five-stranded β-sheet surrounded by three or four α-helices (and a hood domain) (see, for example, Tomchick *et al.*, 1998). Quinolinate PRT comprises a type II fold with two domains: a mixed α/β N-terminal domain and an $\beta_7\alpha_6$ barrel C-terminal domain, similar to known $(\beta\alpha)_8$ barrels (Eads *et al.*, 1997). Anthranilate PRT is predicted to give a typical $(\beta\alpha)_8$ barrel fold (Wilmanns & Eisenberg, 1993). Since there is no similarity in sequence or secondary-structure prediction of ATP-PRT with these PRTs or other known protein structures, we intend to solve the structure by multiwavelength anomalous dispersion (MAD).

6. Quaternary structure model of ATP-PRT

A quaternary structure model of ATP-PRT based on the crystallographic data can be proposed if we assume that the enzyme in the crystal is in a hexameric arrangement (in the presence of the inhibitor AMP) as shown by light scattering (this report), gel separation (Tebar *et al.*, 1973) and ultracentrifugation studies (Klungsøyr & Kryvi, 1971). Taking into account one molecule per asymmetric unit, the symmetry in the hexamer has to be in accordance to the crystallographic symmetry of space group *R*32. Therefore, the twofold and threefold symmetry in this space group must be reflected by the quaternary structure model. The proposed model can be seen in Fig. 3.

Crystal structures of all type I PRTs show a dimeric arrangement (Tomchick *et al.*,

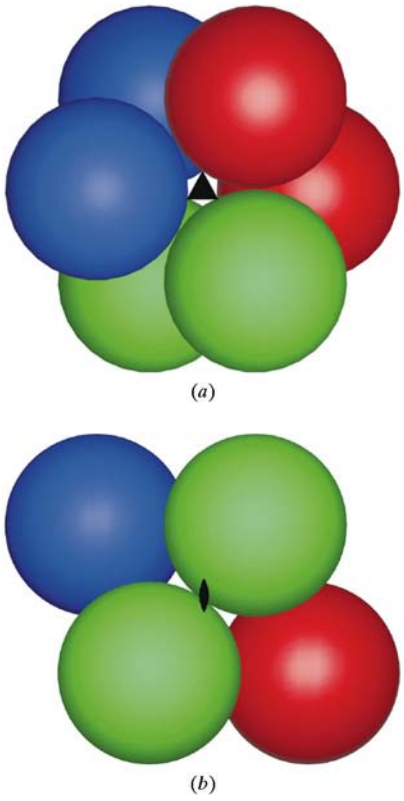

Figure 3
Proposed model of quaternary structure of ATP-PRT. (*a*) shows a view of the hexameric arrangement down the threefold axis. (*b*) is the view along the twofold axis, which is (*a*) rotated 90° towards the viewer. Dimers are indicated by the same colour. Threefold symmetry is marked by *s* and twofold symmetry by *t*.

1998) and uracil PRT shows a hexameric arrangement in solution (Jensen & Mygind, 1996). Therefore, the proposed model of ATP-PRT with dimers arranged within a hexamer is in accordance with known structures of other PRTs.

We would like to thank J. Greene for technical assistance, S. Ali for fruitful discussions, S. Campbell for help with purification and P. Emsley, R. Thom and A. Roszak for help with the data collection. BL would like to thank the Wellcome Trust for funding.

References

Alifano, P., Fani, R., Liò, P., Lazcano, A., Bazzicalupo, M., Carlomagno, M. S. & Bruni, C. B. (1996). *Microbiol. Rev.* **60**, 44–69.

Ames, B. N., Martin, R. G. & Garry, B. J. (1961). *J. Biol. Chem.* **236**, 2019–2026.

Argos, P., Hanei, M., Wilson, J. M. & Kelley, W. N. (1983). *J. Biol. Chem.* **258**, 6450–6457.

Cudney, B., Patel, S., Weisgraber, K., Newhouse, Y. & McPherson, A. (1994). *Acta Cryst.* D**50**, 414–423.

Eads, J. C., Ozturk, D., Wexler, T. B., Grubmeyer, C. & Sacchettini, J. C. (1997). *Structure*, **5**, 47–58.

Ferré-D'Amaré, A. R. & Burley, S. K. (1997). *Methods Enzymol.* **276**, 157–166.

Focia, P. J., Craig, S. P. III, Nieves-Alicea, R. N., Fletterick, R. J. & Eakin, A. E. (1998). *Biochemistry*, **37**, 15066–15075.

Jancarik, J. & Kim, S.-H. (1991). *J. Appl. Cryst.* **24**, 409–411.

Jensen, K. F. & Mygind, B. (1996). *Eur. J. Biochem.* **240**, 637–645.

Klungsøyr, L. & Kryvi, H. (1971). *Biochim. Biophys. Acta*, **227**, 327–336.

Kryvi, H. (1973). *Biochim. Biophys. Acta*, **317**, 123–130.

Kryvi, H. & Klungsøyr, L. (1971). *Biochim. Biophys. Acta*, **235**, 429–434.

Martin, R. G., Berberich, M. A., Ames, B. N., Davis, W. W., Goldberger, R. F. & Yourno, J. D. (1971). *Methods Enzymol.* **17B**, 3–44.

Matthews, B. W. (1968). *J. Mol. Biol.* **33**, 491–497.

Mori, I., Fonné-Pfister, R., Matsunaga, S., Tada, S., Kimura, Y., Iwasaki, G., Mano, J., Hatano, M., Nakano, T., Koizumi, S., Scheidegger, A., Hayakawa, K. & Ohta, D. (1995). *Plant Physiol.* **107**, 719–723.

Mousdale, D. M. & Coggins, J. R. (1991). *Target Sites for Herbicide Action*, edited by R. C. Kirkwood, pp. 29–56. New York: Plenum Press.

Otwinowski, Z. & Minor, W. (1997). *Methods Enzymol.* **276**, 307–326.

Studier, F. W. & Moffatt, B. A. (1986). *J. Mol. Biol.* **189**, 113–130.

Tebar, A. R., Fernandez, V. M., MartinDelRio, R. & Ballestero, A. O. (1973). *Experientia*, **29**, 477–1479.

Tomchick, D. R., Turner, R. J., Switzer, R. L. & Smith, J. L. (1998). *Structure*, **6**, 337–350.

Voll, M. J., Appella, E. & Martin, R. G. (1967). *J. Biol. Chem.* **242**, 1760–1767.

Wilmanns, M. & Eisenberg, D. (1993). *Proc. Natl Acad. Sci. USA*, **90**, 1379–1383.